JOURNAL OF CATALYSIS **168,** 75–94 (1997)
ARTICLE NO. CA971617

Isobutane Dehydrogenation on Pt–Sn/SiO_2 Catalysts: Effect of Preparation Variables and Regeneration Treatments

S. M. Stagg,* C. A. Querini,† W. E. Alvarez,*,[1] and D. E. Resasco*,[2]

*University of Oklahoma, Norman, Oklahoma 73072; and †INCAPE Institute, Santa Fe, Argentina

Received August 23, 1996; revised January 27, 1997; accepted January 27, 1997

The dehydrogenation of isobutane was studied under severely deactivating conditions, i.e., high temperatures and in the absence of added H_2, over silica-supported Pt–Sn catalysts. Several preparation methods were investigated. It was found that the impregnation method employed has a strong influence on the degree of Pt–Sn interaction and the fraction of Pt that remains unalloyed after the calcination and reduction process. The co-impregnation methods investigated were significantly superior to the sequential method. It was found that it is important to minimize the amount of unalloyed Pt left on the catalyst because this fraction rapidly forms coke and deactivates. At the same time, the fraction of unalloyed Pt, rather than the one alloyed with Sn, is responsible for most of the CO and hydrogen adsorbed at room temperature in typical chemisorption measurements. As a consequence, the TOF values based on this type of measurements are in error because they are not related to the density of sites that are responsible for long term activity. It was also found that the high-temperature reduction/oxidation treatments usually employed to regenerate spent catalysts can have a detrimental effect on the activity and selectivity of the Pt–Sn/SiO_2 catalysts. It is postulated that such thermal treatments lead to the disruption of the Pt–Sn alloys causing an increase in the fraction of unalloyed surface Pt. As a result, the rates of coke formation and deactivation drastically increase. The monometallic (Pt only) catalysts are also affected by the high-temperature reduction/oxidation processes. The oxidation treatment results in an increased rate of coke formation and deactivation, while the regeneration process results in a much smaller effect. This difference may be due to carbon residues left on the surface. These residues may disrupt Pt ensembles and cause a decrease in the rate of undesired reactions, such as hydrogenolysis and coking, that require a large ensemble of Pt atoms.

INTRODUCTION

Recent increases in demand of light olefins for the production of polymers and gasoline additives such as MTBE have increased the interest in lower alkane dehydrogenation (1). The conditions best suited for this reaction, high temperatures, low pressures, and low hydrogen concentrations, favor rapid deactivation due to coke formation on the catalyst. On Pt-based catalysts, it is sometimes necessary to add hydrogen to the feed to reduce deactivation. However, in commercial applications, the use of high hydrogen/hydrocarbon feed ratios is highly undesirable because the equilibrium conversion decreases and the compression costs greatly increase.

Research has found that the addition of promoters, such as Sn, to Pt catalysts enhances their catalytic ability for dehydrogenation (2, 3). One explanation for the enhanced properties of the promoted catalysts is the formation of alloys between the Pt and the Sn which reduces the size of Pt ensembles (4, 5), decreasing coke formation and increasing selectivity. It has also been suggested that Sn may modify the catalytic properties of Pt by electronic or ligand effects (6, 7). This modification may be responsible for changes in the heat of adsorption of different adsorbates participating in the reaction (8, 9).

Even though Sn is one of the most efficient promoters employed in commercial processes (10, 11), deactivation due to coke formation is not completely eliminated and the catalysts still exhibit short lifetimes and must undergo continuous or frequent regenerations to maintain activity (12). The regeneration typically consists of exposing the spent catalyst to oxygen or air at high temperatures to burn off any carbon produced during the reaction, followed by a reduction step that brings the catalyst back to the active (metallic) form.

One of the issues that we explore in this contribution is the possibility that the exposure to such reduction/oxidation cycles can cause important changes in the catalyst morphology that negatively alter the catalytic properties of the bimetallic catalyst. For example, studies have shown that Pt–Rh alloys, when heated in air, form particles with Pt-rich centers and Rh_2O_3 outer surface (13, 14). Subsequent reduction results in a metallic Rh layer covering a Pt core (15). On the other hand, Pt–Pd supported alloys behave differently when heated in air at high temperatures. Oxidation causes the Pt–Pd alloy to form two separate

[1] Permanent address: INTEMA, University of Mar del Plata, Argentina.
[2] To whom correspondence should be addressed. Fax: (405) 325-5813. E-mail: resasco@ou.edu.

0021-9517/97 $25.00

crystallites of metal and PdO, both in contact with the silica support (16). When reduced at high temperatures, the Pd forms metal particles on the edges of the Pt particle. Work has also been done on Pt–Ir alloys, and it has been shown that the alloy is completely destroyed when heated in air (17, 18). For the particular case of Pt–Sn, Verbeek and Sachtler (7) proposed that, after exposure to air and subsequent reduction, the unsupported Pt–Sn alloys become surface enriched in Sn at the expense of the subsurface zone, with the center of the particle getting rich in Pt. More recently, Chojnacki and Schmidt (19) studied Pt–Sn films supported on planar amorphous silica films and found that exposure to O_2 at 550°C for 1 h resulted in destruction of the intermetallic species leaving metallic Pt cores surrounded by a ring of SnO_2 in contact with the silica. However, after subsequent reduction for long periods of time (18 h at 650°C), complete recombination of the alloys was obtained.

The aim of this paper is to study the interaction between the active metal (Pt) and the promoter (Sn) following different preparation methods, as well as the effects of regeneration treatments on catalytic properties. By using a combination of characterization techniques and catalytic activity measurements, we have studied three different Pt–Sn bimetallic catalysts and analyzed the extent of metal–metal interaction. It is widely recognized that the support can strongly affect the metal–metal interaction (20), and if it contains acidity, it can greatly promote the rate of coke formation under isobutane dehydrogenation conditions (21). Therefore, we have used a silica support which interacts very weakly with Pt or Sn and does not contain acidity. We have found that on this support, the fraction of Pt that becomes alloyed with Sn strongly depends on the preparation method. This fraction in turn has a strong influence on the catalytic performance and can be significantly altered under conditions typically encountered during regeneration.

We have also found that the standard method used to report turnover frequencies cannot be applied to the bimetallic Pt–Sn catalysts because the fraction of unalloyed Pt which is responsible for the adsorption of H_2 or CO, generally used as probes to count sites, rapidly deactivates under reaction conditions. The rapid deactivation of unalloyed Pt is particularly important in the absence of added hydrogen.

EXPERIMENTAL

Catalyst Preparation

Pt and Pt–Sn catalysts were supported on SiO_2 (W. R. Grace & Co., Silica Gel Grade 923). Table 1 shows the characteristics of the catalysts investigated. They were prepared by incipient wetness impregnation using $SnCl_2 \cdot 2H_2O$ and either $H_2PtCl_6 \cdot 6H_2O$ or $Pt(NH_3)_4(NO_3)_2$ as the precursors for the metals. The incipient wetness liquid/solid ratio was determined for each preparation and varied from 0.5 to 0.75 cc/g. Two monometallic Pt samples, (1.5 wt%) and (1.0 wt%), were prepared by incipient wetness impregnation. The 1.5 wt% Pt was prepared using an aqueous solution of $H_2PtCl_6 \cdot 6H_2O$, while for the 1.0 wt% Pt catalyst, a HCl solution was used as the solvent. The bimetallic catalysts were prepared by three different techniques. One sample was made by co-impregnation with an aqueous solution containing a 1 : 1 molar ratio of Pt : Sn and will be referred to as CI. A second set of catalysts was prepared by sequential impregnation (SI) of Pt followed by Sn. In this case, $Pt(NH_3)_4(NO_3)_2$ was dissolved in water while the Sn salt was dissolved in acetone. The two sequentially impregnated samples will be referred as SI0.3 (0.3 wt% Pt and 0.3 wt% Sn) and SI1 (1 wt% Pt and 1 wt% Sn). The third technique used was co-impregnation of 1 wt% Pt and 1 wt% Sn with a HCl solution as the solvent and will be referred to as CIC. It has been shown (22) that, in the presence of HCl, a bimetallic complex $PtCl_2(SnCl_3)_2^{2-}$ is formed in solution and a higher degree of metal–metal interaction should result. The impregnated samples were dried overnight at 110°C and stored.

Subsequently, all catalysts were exposed to cycles of reduction/oxidation before characterization and activity tests. The treatments and nomenclature, summarized in Table 2, are as follows. The term "fresh" is applied to impregnated samples which were calcined in air at 400°C for 2 h. Regenerated samples had initially the same pretreatment as the fresh ones, but then were reduced in H_2 at 500°C for 1 h, exposed to isobutane at 500°C, and treated in air for 1 h at 300, 400, or 500°C to burn any carbonaceous deposits that formed during reaction. These catalysts will be referred to as REG300, REG400, and REG500, respectively. Some

TABLE 1

Characteristics of the Catalysts Investigated

Catalyst nomenclature	Pt (wt%)	Molar Pt : Sn ratio	Preparation techniques	Solvent	Precursor
Pt (1.0)	1.0	1 : 0	Impregnation	HCl	H_2PtCl_6
Pt (1.5)	1.5	1 : 0	Impregnation	Water	H_2PtCl_6
Pt–Sn (CI)	1.5	1 : 1	Co-impregnation	Water	H_2PtCl_6
Pt–Sn (CIC)	1.0	1 : 1.65	Co-impregnation	HCl	H_2PtCl_6
Pt–Sn (SI0.3)	0.3	1 : 1.65	Sequential impregnation	Acetone	$Pt(NH_3)_4(NO_3)_2$
Pt–Sn (SI1)	1.0	1 : 1.65	Sequential impregnation	Acetone	$Pt(NH_3)_4(NO_3)_2$

TABLE 2

Summary of the Different Pretreatments Performed on the Catalysts

Pretreatment nomenclature	Conditions
Fresh	Calcined in air at 400°C for 2 h
REG300, REG400, REG500	Fresh sample reduced in H_2 at 500°C for 1 h, exposed to reaction conditions at 500°C for 1 h, and then exposed to air at 300, 400, and 500°C, respectively, for 1 h
OX300, OX400, OX500	Fresh sample reduced in H_2 at 500°C for 1 h and exposed to air at 300, 400, and 500°C, respectively, for 1 h

fresh samples were reduced and then oxidized in air for 1 h at 300, 400, and 500°C without exposure to isobutane. These samples will be referred to as OX300, OX400, and OX500, respectively.

Catalyst Characterization

Volumetric H_2 chemisorption measurements were performed using a Micromeritics ASAP 2000 system. For each measurement, 0.6 g of each catalyst was loaded into the chemisorption cell. The sample was reduced *in situ* at 500°C for 1 h, evacuated to 10^{-6} Torr at 500°C, and then cooled to 35°C at which the adsorption of H_2 was performed. Chemisorption capacities were measured on fresh, OX300, OX400, and OX500 samples of Pt (1.5) and Pt–Sn (CI), as well as on fresh Pt–Sn (CIC).

Dynamic CO chemisorption measurements were carried out by sending 250-μl pulses of 5% CO/He on 0.3-g samples of either fresh catalysts, after reduction in H_2 for 1 h at 500°C, or catalysts that had been exposed to reaction conditions. The He used as a carrier and to purge the catalyst was purified through a MnO trap before contacting the sample. A methanator reactor that quantitatively transforms CO in CH_4 was employed to increase the sensitivity of the CO analysis. A FID detector was used to continuously monitor the CH_4. Details of this technique can be found elsewhere (23). To determine the CO adsorption capacity, consecutive pulses were sent until the amount of CO leaving the sample was the same as that by-passing the sample. The adsorption capacity (CO/Pt) was calculated from the sum of the differences between the by-pass and each pulse.

Transmission electron microscopy (TEM) was performed on fresh and OX500 samples of a bimetallic catalyst with Pt : Sn ratio of 1 : 1. Each sample was reduced at 500°C for 1 h, cooled in He to room temperature, and then slowly exposed to air overnight. The catalyst was then ground into a fine powder and suspended in isopropyl alcohol. One drop of solution was placed on a 0.3-mm-diameter Lacey carbon grid (Electron Microscopy Sciences) and allowed to dry. All samples were analyzed using a JEOL 2000FX TEM.

Temperature-programmed reduction (TPR) experiments were performed on fresh samples of Pt, Pt–Sn (CI), Pt–Sn (CIC), and Pt–Sn (SI) in an OKHURA TP-2002S system. In addition, TPRs were performed on OX300, OX400, OX500, and REG500 samples of Pt (1.5) and Pt–Sn (CI). The sample weight varied from 0.25 to 0.34 g; therefore, all signals have been normalized to a per gram basis. The TPR runs were conducted using a heating rate of 10°C/min in a flow of 5% H_2/Ar (45 cc/min) up to 800°C. A zeolite trap was used to eliminate water during the TPR.

Temperature-programmed oxidation (TPO) experiments of carbonaceous deposits deposited under reaction conditions were conducted on the Pt (1.5) and Pt–Sn (CI) catalysts. Samples consisting of 0.1 g were heated to 500°C in a H_2 flow (100 cc/min). At 500°C, each sample was exposed to isobutane or mixtures of isobutane/H_2/He for 15 min and then cooled to room temperature in He. Once at room temperature, the sample was heated at a rate of 8°C/min in O_2 (30 cc/min) up to 800°C. TPOs of carbonaceous deposits were also performed on fresh Pt (1.5) and Pt–Sn (CI) samples after exposure to pure isobutane for 2 min. The heating rate was 8°C/min in a 5% O_2/He mixture (30 cc/min). The exit gases were analyzed using a quadrupole residual gas analyzer from MKS. In order to normalize the pressure data, 200 μl of CO_2 was injected three times when the system reached 800°C and the average peak area for the injections was determined. The amount of coke formed on the catalysts under various conditions was determined using the known moles of CO_2 and the area of the injections.

Catalyst Activity

The isobutane dehydrogenation activity was measured in a flow reactor consisting of a quartz tube with an inner diameter of 0.4 cm and an outer diameter of 0.6 cm. Samples consisting of 0.015 g of each catalyst were loaded into the quartz reactor, supported on both sides by quartz wool. The samples were reduced *in situ* at 500°C for 1 h and then contacted with the feed gas containing varying concentrations of isobutane in He. The majority of the runs were conducted in the absence of H_2, using a 2 : 1 isobutane : He ratio, at a flow rate of 36 cc/min, which resulted in a space velocity of 248 WHSV. The exit gases were analyzed in a Hewlett Packard GCD equipped with a quadrapole mass analyzer which identified all species generated during the reaction. The conversion was calculated from the area of the isobutene peak divided by the sum of the areas of all the species detected. The selectivity was calculated from the area of the isobutene peak divided by the sum of the areas of all the products.

To ensure that no heat transport problems occurred, thermocouples were placed in direct contact with the top and bottom of the bed during the reaction. In addition, a third thermocouple was placed at the side of the bed which was used to control the temperature of the furnace.

The temperature drop across the bed was measured during the runs, and the largest ΔT observed was less than 2°C. For a typical activation energy of 20 kcal/mol, this difference, measured at the highest conversion (approximately 35%) would represent a maximum error of ±1% conversion, which is much less than the typical variations in activity due to any of the effects that we have considered in the paper. Similarly, from the application of the Wiesz–Prater criteria for internal diffusion, we have concluded that mass transfer limitations were not present in our experiments.

RESULTS

H_2 and CO Chemisorption

Table 3 gives the H_2 chemisorption data obtained for fresh samples of Pt (1.5), Pt–Sn (CI), and Pt–Sn (CIC) catalysts, as well as OX300, OX400, and OX500 Pt (1.5) and Pt–Sn (CI) catalysts. As shown in Table 3, the bimetallic catalysts Pt–Sn (CI) and, particularly, Pt–Sn (CIC) exhibited significantly lower chemisorption capacities than the monometallic catalysts. For the pure Pt (1.5) sample, varying the oxidation temperature resulted in only a small variation in the fraction of Pt exposed. The Pt–Sn (CI) sample showed an initial decrease in the fraction exposed with oxidation at 300°C followed by little variation in adsorption capacity with increasing oxidation temperature. Chemisorption values on the fresh samples were within the range of values reported in the literature (15, 24, 25).

The CO adsorption studies were performed on fresh and spent Pt (1.5 and 1.0), Pt–Sn (CI), and Pt–Sn (CIC) catalysts. Table 3 shows the amount of CO adsorbed by each catalyst. As in the case of H_2 chemisorption, the monometallic Pt catalysts was found to adsorb much more CO than the bimetallic samples. The Pt–Sn (CIC) catalyst showed slightly less CO adsorption than the Pt–Sn (CI) sample. An interesting result was observed on the spent catalysts. After 1 h under reaction conditions (500°C, pure isobutane, 30 WHSV) the samples were cooled in pure He and tested by dynamic CO adsorption. As shown in Table 3, the adsorption capacity of the bimetallic samples, particularly Pt–Sn (CIC), became exceedingly low. It is important to note that, despite losing their chemisorption capacity, these samples still retained most of their original activity.

TABLE 3

Hydrogen and CO Chemisorption and Initial Turnover Frequencies

				Turnover frequencies (sec^{-1})		
		Chemisorption				
Catalyst	Pretreatment	H/Pt	CO/Pt	Based on H/Pt	Based on CO/Pt	Per total Pt
Pt (1.5)	Fresh	0.51	0.38	2.2	3.6	1.12
	OX300	0.58	—	2.3	—	—
	OX400	0.56	—	—	—	—
	OX500	0.49	—	2.4	—	—
	Spent	—	0.13	—	—	—
Pt (1.0)	Fresh	—	0.3	—	—	—
	Spent	—	0.03	—	—	—
Pt–Sn (CI)	Fresh	0.30	0.1	6.2	20.6	1.86
	OX300	0.21	—	7.9	—	—
	OX400	0.24	—	7.1	—	—
	OX500	0.22	—	4.5	—	—
	Spent	—	0.02	—	—	—
Pt–Sn (CIC)	Fresh	0.09	0.06	30.9	46.3	2.78
	Spent	—	<0.01	—	—	—

Transmission Electron Microscopy

Figures 1a and 1b show the TEM images of a coimpregnated 1 : 1 Pt : Sn catalyst. The micrographs represent respectively the fresh and OX500 samples after reduction in H_2 at 500°C for 1 h. The fresh sample showed two types of particles. The first range from 25–50 Å in size and were very light in contrast. The second type were much larger (150–250 Å) and much darker in contrast. After treatment in air at 500°C for 1 h and reduction for 1 h, both types of particles underwent changes. The small particles experienced growth so that the average particle size became 50–100 Å. The larger particles also experienced morphological changes so that the contrast of the particles was no longer homogeneous. The particles consisted of surfaces of light contrast with distinct patches of darker contrast. The monometallic Pt catalyst exhibited smaller particles (20–30 Å), consistent with the dispersion values determined by the chemisorption measurements.

Temperature-Programmed Reduction

Figure 2 shows the results of the TPR studies done on the pure Pt (1.5) and Pt–Sn (CIC) catalysts after calcination at 350°C. The TPR for the pure Pt catalyst shows that the H_2 consumption has a maximum at about 125°C and ends at about 200°C. This profile also shows some H_2 consumption at about 400°C. However, this is not due to the reduction of Pt species, but rather to the removal of impregnation precursors which were not totally eliminated during the initial calcination step. The profile for the Pt–Sn (CIC) catalyst has two H_2 consumption peaks. The first appears in the same position as that for pure Pt (125°C), while the second has a maximum at 200°C. Unlike the catalysts prepared by sequential impregnation, the Pt–Sn (CIC) shows no reduction peak at high temperatures, characteristic of unalloyed Sn.

The profiles for the Pt–Sn (Si0.3) catalysts are shown in Fig. 3. They contain peaks that are broader and extend to much higher temperatures than those shown in Fig. 2. Calcination of the sample at 400°C resulted in three H_2 consumption regions. The first peak again appears at the same position as that for pure Pt (125°C) and has the smallest

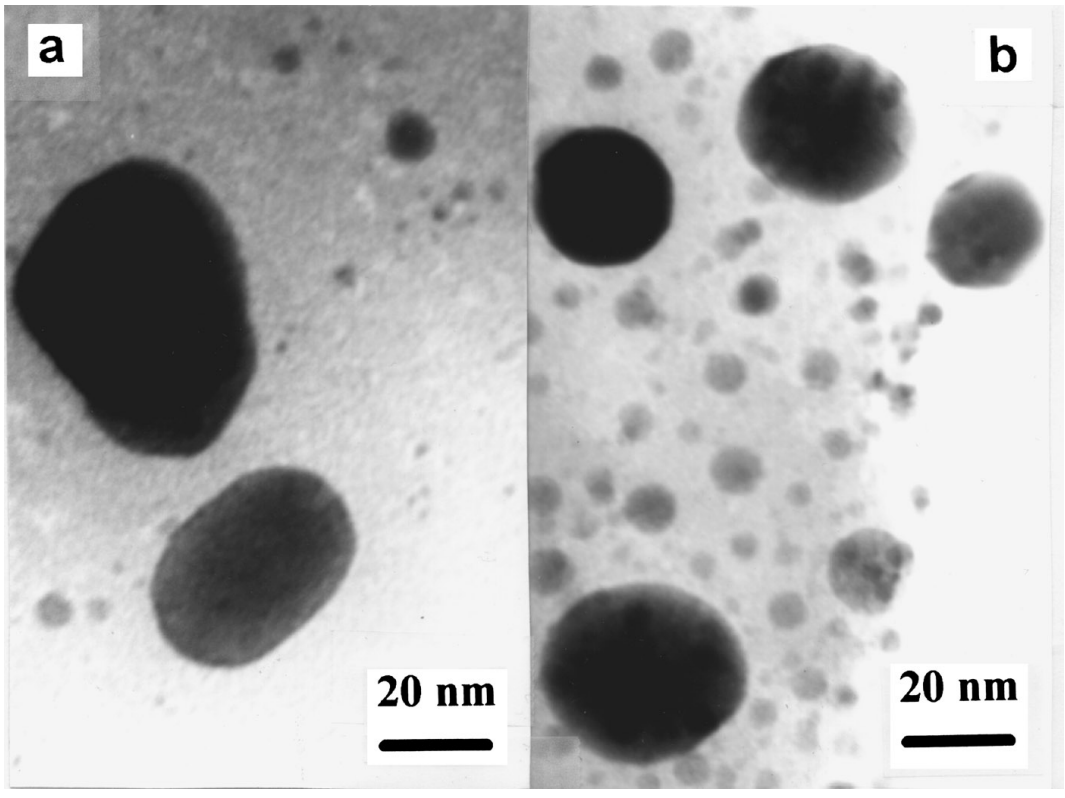

FIG. 1. TEM micrographs of co-impregnated silica-supported Pt–Sn catalyst (1 wt% Pt, 1 wt% Sn) (a) fresh after reduction and (b) OX500 after reduction.

intensity of the three peaks. The second consumption region is the largest and has a maximum near 250°C. The last region spans from approximately 400 to 600°C with the greatest intensity at about 525°C. Figure 3 also shows the consequences of increasing the calcination temperature on the TPR profile. When the calcination was done at 500°C for 2 h, the peak at 125°C did not change much, but the peak at 250°C decreased in intensity while the higher temperature peak became dominant. Also, the position of the third region shifted slightly so that the maximum occurred at

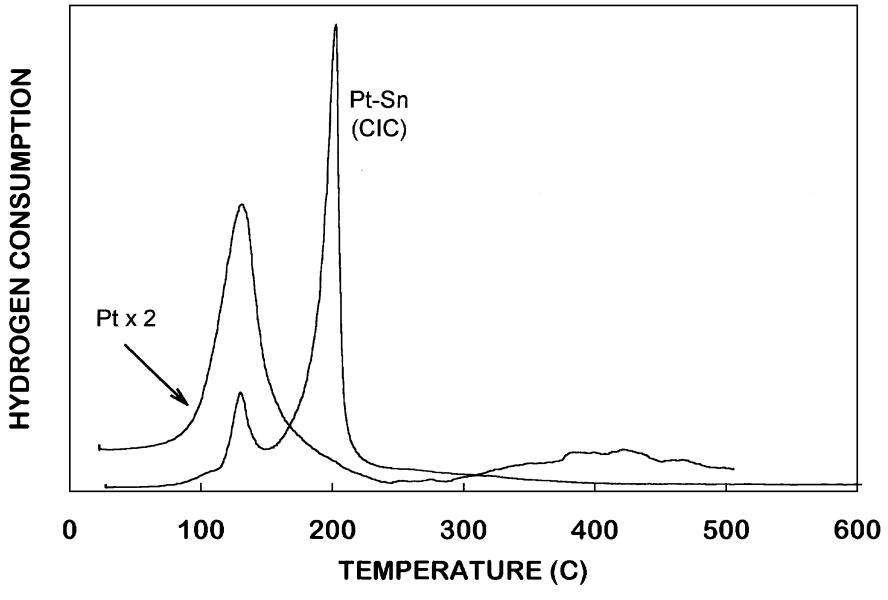

FIG. 2. Temperature-programmed reduction (TPR) profiles of silica-supported Pt (1.5) and Pt–Sn (CIC) catalysts after calcination at 350°C.

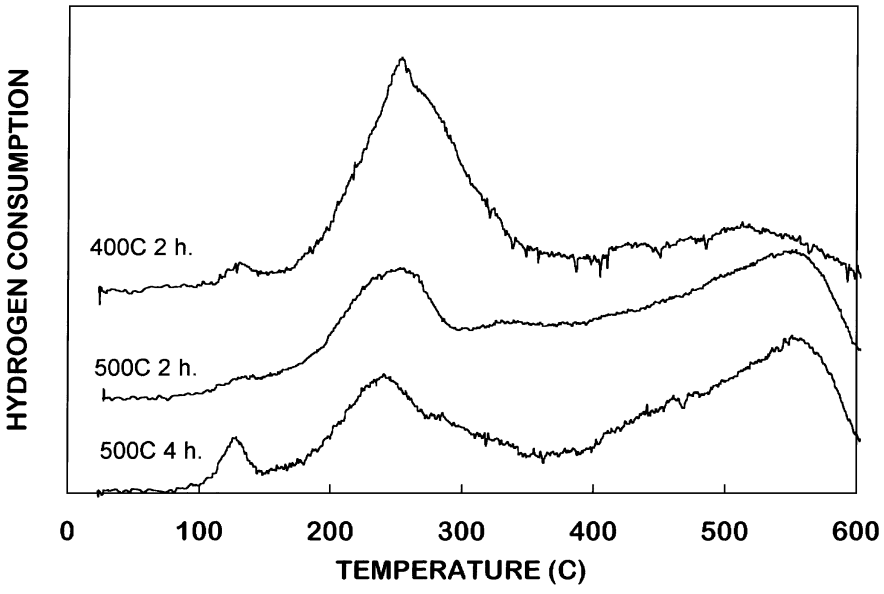

FIG. 3. TPR profiles of silica-supported Pt–Sn (Si0.3) catalyst after calcination at various temperatures and times.

575°C. When the calcination time increased to 4 h, the low-temperature region showed a large increase in intensity.

The TPR profiles for the Pt–Sn (CI) catalyst after oxidation at different temperatures are shown in Fig. 4. The fresh Pt–Sn (CI) sample showed three hydrogen consumption peaks centered at 146, 186, and 375°C. The first two peaks appeared as a large broad region with the highest intensity at 186°C and a shoulder at lower temperatures. The third peak was much smaller. Subsequent oxidation of the reduced sample at 300, 400, and 500°C resulted in the removal of the high-temperature peak and, more relevant to the succeeding discussion, a significant decrease in the intensity of the peak at 186°C. This decrease in intensity was accompanied by the appearance of a shoulder between 200 and 300°C that made the peak broader. Finally, the peak that appeared at 146°C on the fresh sample slightly changed position as the oxidation temperature increased. A comparable set of experiments was done for the pure Pt (1.5) catalyst (not shown). These runs exhibited a single consumption peak at about 125°C which did not change much after the various oxidation pretreatments. These runs confirmed that the peak at about 400°C in the fresh monometallic

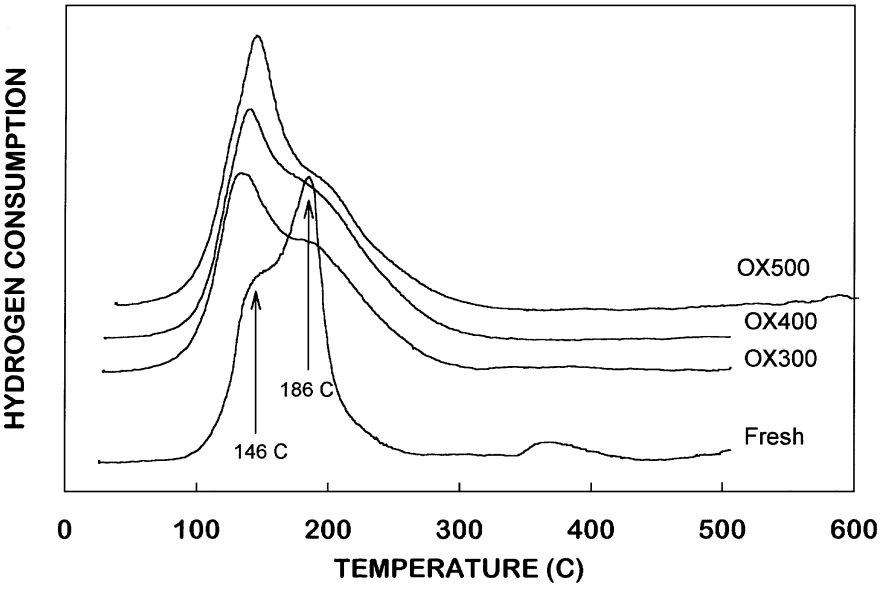

FIG. 4. TPR profiles of the Pt–Sn (CI) catalyst after various pretreatments: fresh, OX300, OX400, and OX500 (see Table 2 for details of each pretreatment).

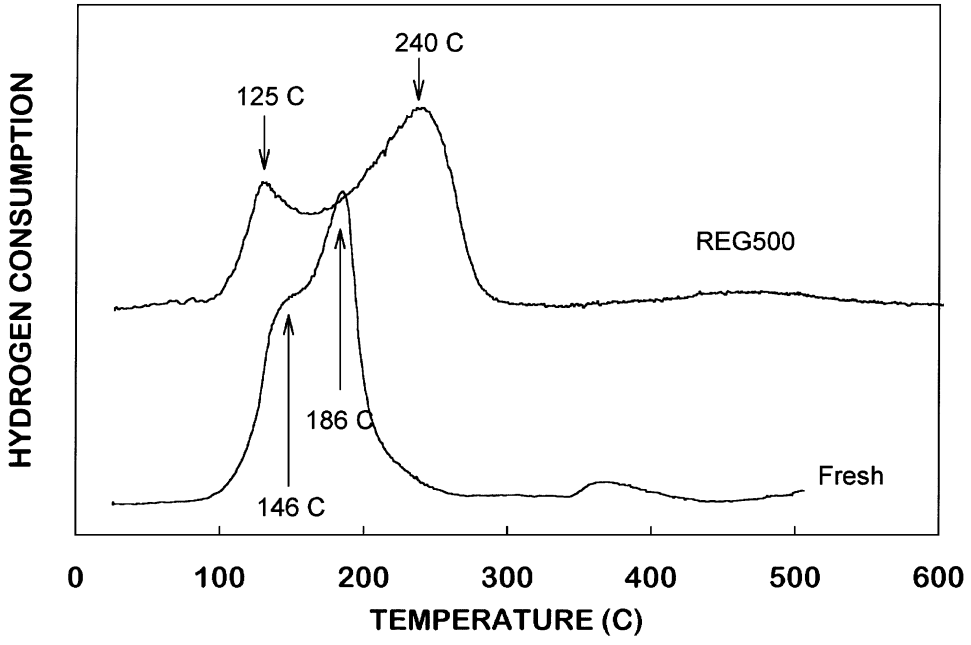

FIG. 5. TPR profiles of the Pt–Sn (CI) catalyst after various pretreatments: fresh and REG500 (see Table 2 for details of each pretreatment).

catalyst was due to the removal of residues from the impregnation precursors. They were eliminated during the reduction/oxidation cycles and the H_2 consumption at 400°C did not appear for these samples.

Figure 5 shows the TPR results for the regenerated Pt–Sn (CI) sample, REG500, in comparison to the fresh catalyst. The result is similar to that observed for the series of oxidized samples, although in this case the effects were more pronounced. The low-temperature peak shifted to the position that is typical of unalloyed Pt, 125°C, while the conversion of the 186°C peak into a broad peak at about 240°C was more evident for this sample than for the oxidized samples.

Temperature-Programmed Oxidation of Carbonaceous Deposits

TPO studies were performed on the catalysts after exposure to isobutane for 15 min. Figure 6 shows that, in agreement with previous studies (4), the addition of Sn decreased

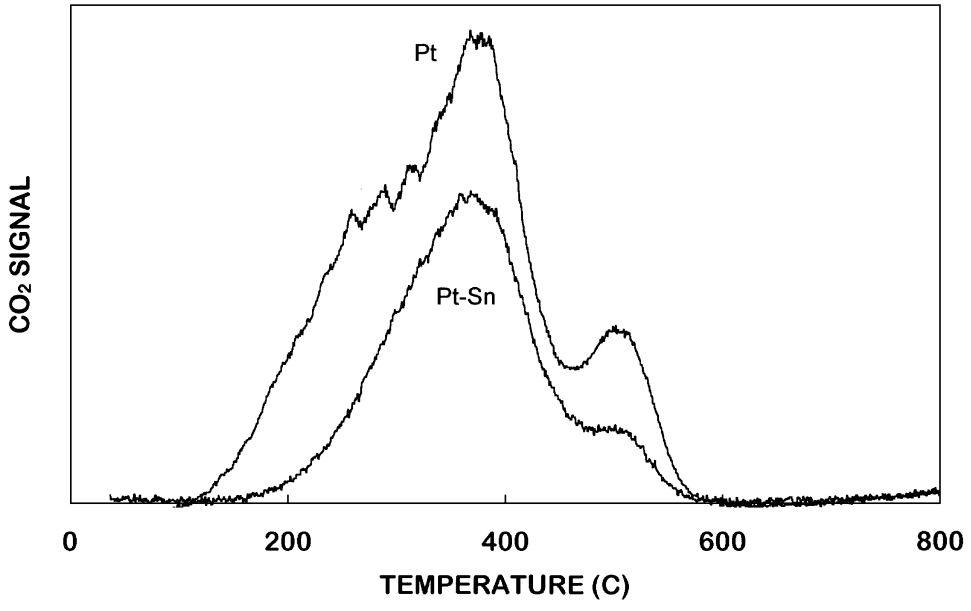

FIG. 6. Temperature-programmed oxidation (TPO) profiles of carbonaceous deposits left on the monometallic Pt (1.5) and the bimetallic Pt–Sn (CI) catalysts after exposure to isobutane at 500°C for 15 min.

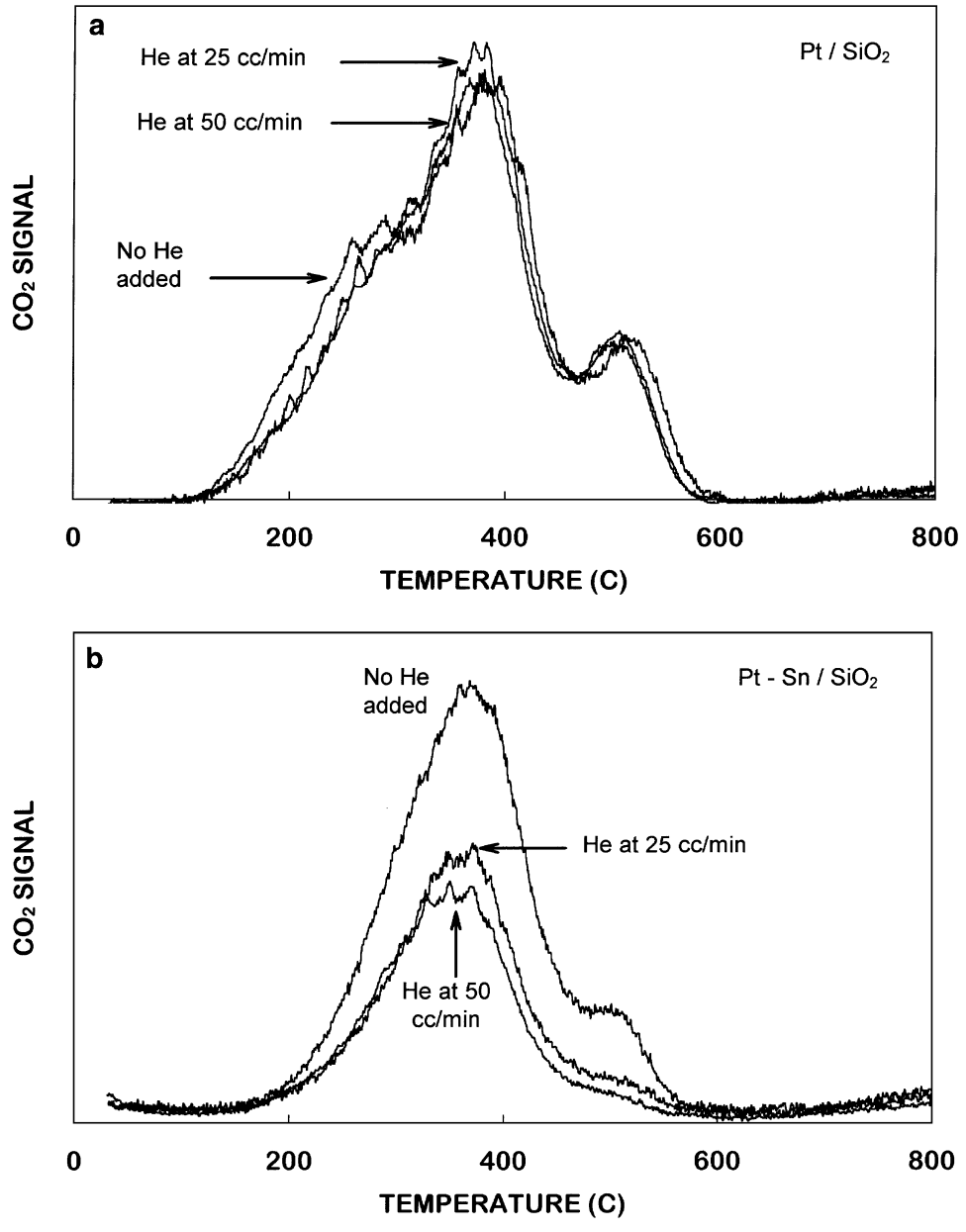

FIG. 7. TPO profiles of carbonaceous deposits left on the catalysts after exposure to isobutane at 500°C for 15 min at a constant isobutane flow rate of 54 cc/min (83 WHSV) and He flow rates of 0, 25, and 50 cc/min. (a) Pt (1.5)/SiO_2 catalyst; (b) Pt–Sn (CI)/SiO_2 catalyst.

the intensity of the CO_2 evolution in all three oxidation regions. The position of the peaks are the same for the pure Pt and bimetallic Pt–Sn samples; however, the amount of coke formed on the bimetallic sample was approximately 50% less than that on the monometallic Pt catalyst. The amount of carbon formed on the Pt (1.5) catalyst after 15 min was 0.31 wt%, which corresponds to about four C atoms per Pt atom.

Figures 7a and 7b show the results of diluting the isobutane feed with He on the Pt (1.5) and Pt–Sn (CI) samples, respectively. On the Pt catalyst, dilution with He had almost no influence on the amount of coke measured after 15 min of reaction. However, on the Pt–Sn (CI) dilution with He resulted in the reduction of the largest TPO peak (375°C) by about 50% and almost complete elimination of the high-temperature oxidation peak (510°C). Dilution with He did not affect the position of any of the three oxidation peaks for either the Pt (1.5) or the Pt–Sn (CI) catalysts.

Changing the partial pressure of isobutane with the addition of H_2 modified the coke formation for both the Pt (1.5) and the Pt–Sn (CI) catalysts. Figures 8a and 8b show that the intensity of all of the peaks decreased by about 50% when the ratio of H_2 to isobutane approached 1. Also, the high-temperature peak showed a slight shift in temperature

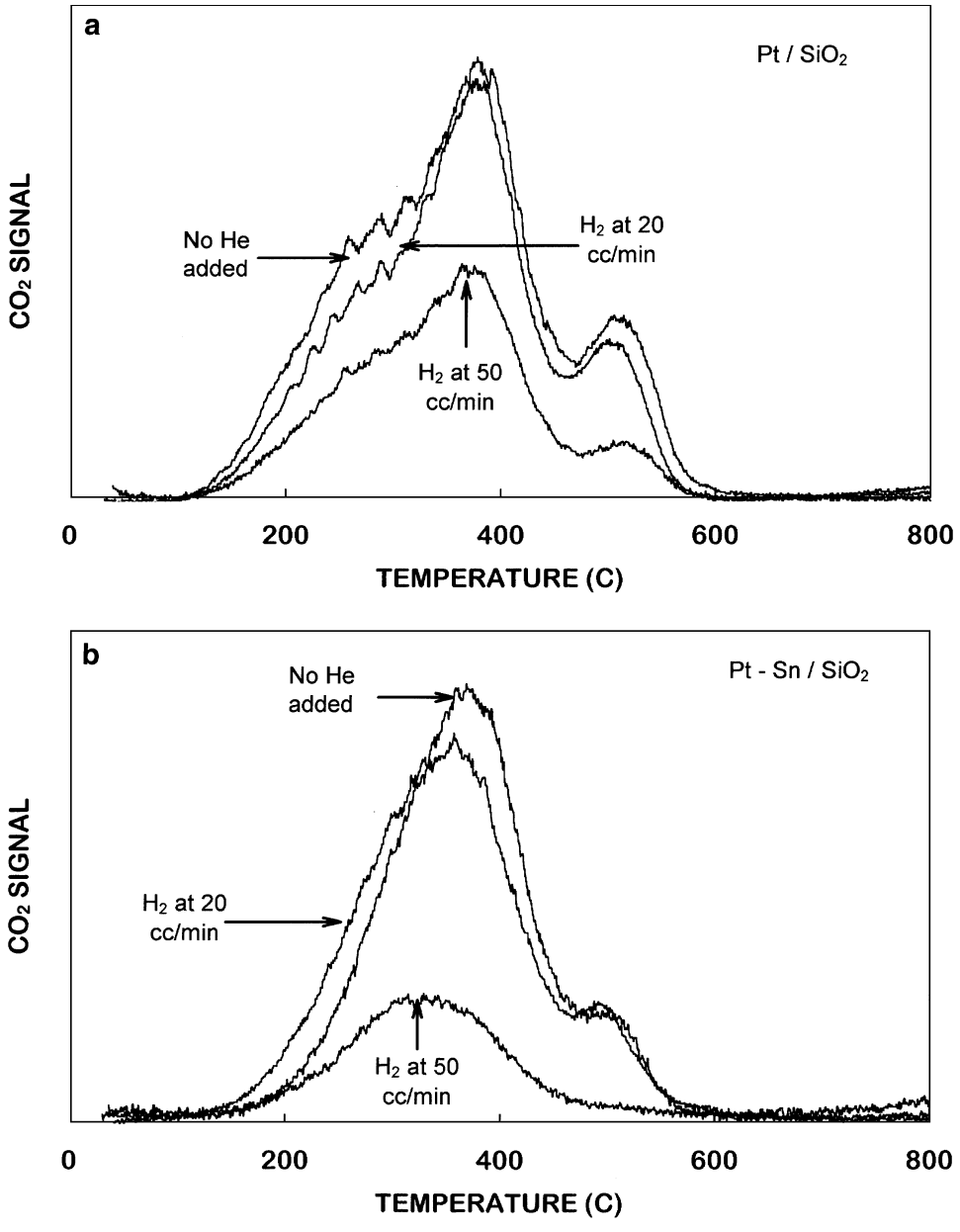

FIG. 8. TPO profiles of carbonaceous deposits left on the catalysts after exposure to isobutane at 500°C for 15 min at a constant isobutane flow rate of 54 cc/min (83 WHSV) and H_2 flow rates of 0, 25, and 50 cc/min. (a) Pt (1.5)/SiO_2 catalyst; (b) Pt–Sn (CI)/SiO_2 catalyst.

from a maximum of 500°C with no H_2 flow to 525°C at a H_2 flow of 50 cc/min. The Pt–Sn (CI) catalyst showed changes in both the intensity and the positions of the peaks with the addition of H_2. The largest peak shifted from approximately 375°C with no H_2 flow to 325°C with H_2 flow of 50 cc/min. The high-temperature peak was not affected with a H_2 flow of 20 cc/min but was completely removed at the higher flow rate of H_2. Figure 9 compares the amount of carbon deposited on each catalyst for the various conditions described above. The trend lines clearly show the effects of adding H_2 and He to the feed stream along with the reduction in coke formation with the addition of Sn. It is observed that dilution with He does not affect the amount of coke deposited on the monometallic catalyst. Deactivation of the Pt catalyst occurs so rapidly that saturation of the surface by carbon deposits has occurred after only a few minutes on stream. However, dilution with hydrogen results in a marked decrease in the amount of carbon when the H_2 : hydrocarbon ratio approaches 1 : 1 due to hydrogenation of coke precursors.

Figure 10 shows the TPO profiles for three Pt (1.5) samples after exposure to pure isobutane for 2 min. The first is

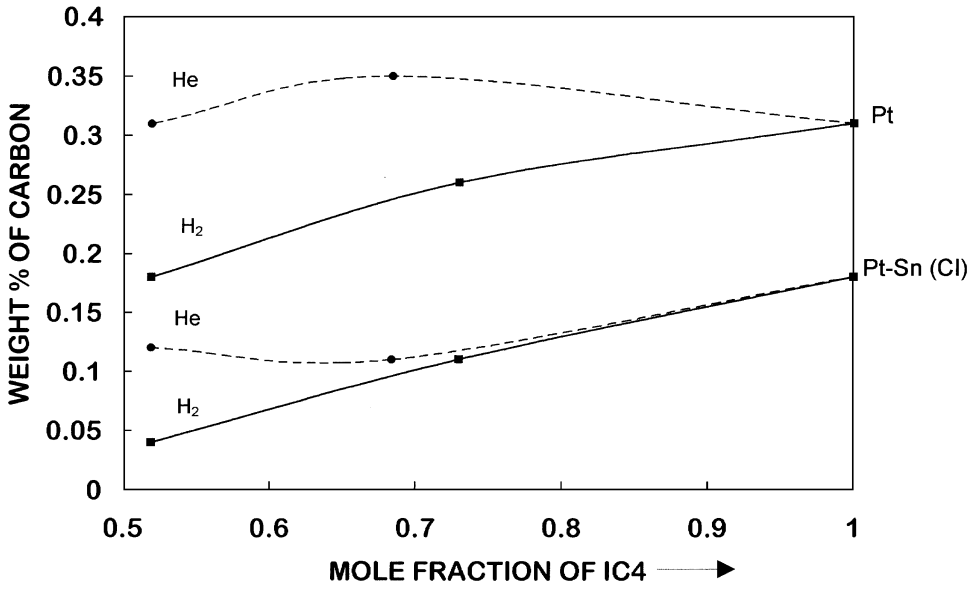

FIG. 9. Amount of carbon deposited on the Pt (1.5) and Pt–Sn (CI)/SiO_2 catalysts, after 15-min exposure to isobutane at 500°C and at a space velocity of 83 WHSV, as a function of isobutane concentration in He (circles) and H_2 (squares).

a fresh sample exposed to isobutane at 500°C for 2 min. The second is OX500 which has been exposed to isobutane for 2 min at 500°C. The third is a fresh sample which has been exposed to isobutane for 2 min at 500°C, regenerated in air at 500°C for 1 h, reduced in H_2 at 500°C for 1 h, and then exposed to isobutane a second time for 2 min (REG500). Since the amount of coke is a strong function of the olefin concentration in the gas phase and, consequently, the level of conversion, we have normalized the TPO signal to the steady-state conversion obtained on each of the samples. All comparisons will be made on this basis.

The TPO profile for the fresh sample of the monometallic Pt (1.5) catalyst after 2 min of reaction is similar to the one obtained after 15 min of reaction. Oxidation at 500°C before exposure to reaction caused the position of the CO_2 peaks to shift to higher temperatures. The appearance of a high-temperature oxidation peak was seen on the oxidized catalyst, but this peak was not present on the regenerated

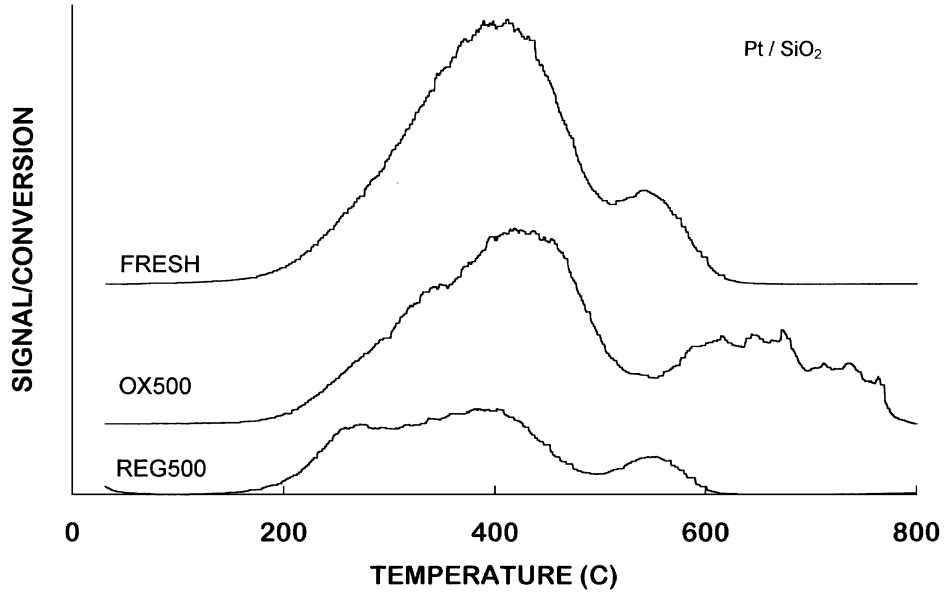

FIG. 10. TPO profiles of fresh, OX500, and REG500 samples of pure Pt (1.5)/SiO_2 catalysts after exposure to isobutane at 500°C (248 WHSV) for 2 min.

sample. This high-temperature peak started at approximately 550°C and spanned up to 800°C. The two peaks at lower temperatures shifted from approximately 275 and 400°C to 350 and 425°C, respectively. The amount of coke formed on the oxidized catalyst was slightly less than that of the fresh sample. Regeneration of the catalyst resulted in a 45% decrease in the coke formed during the second exposure to isobutane. The positions of all three oxidation peaks were identical to that of the fresh sample; however, the intensity of each of the peaks, especially the one at 400°C, was significantly reduced.

As we explain below, we ascribe the reduced rate of coke formation observed on the regenerated catalysts to the presence of coke deposits that were not removed by the regeneration process. These remaining deposits modify the Pt surface making it more resistant to coking. To prove this, we conducted TPO measurements on a regenerated catalyst without further exposure to the isobutane feed. Indeed, this experiment showed that about 25% of the carbon initially deposited still remained on the catalyst after the regeneration step.

Contrary to the monometallic catalyst, the bimetallic Pt–Sn (CI) showed an increase in the rate of coke formation after the regeneration and oxidation pretreatments. As shown in Fig. 11, the fresh sample formed a very low amount of coke during exposure to isobutane for 2 min. Only one broad oxidation peak was observed at approximately 375°C. The OX500 catalyst formed a much larger amount of coke and the subsequent TPO profile looked very similar to that of the oxidized monometallic Pt (1.5) sample. The main peak shifted to temperatures near 410°C and a new high-temperature peak appeared near 650°C. Like the oxidized Pt–Sn catalyst, the regenerated sample (REG500) resulted in a much higher rate of coke formation that the fresh bimetallic catalyst and the TPO of this sample exhibited a single broad peak centered at around 410°C.

In summary, the reduction/oxidation (500°C) cycle on the monometallic Pt catalyst did not have a great effect on the amount of coke formed during the following reaction period but significantly altered its oxidation characteristics, i.e., the coke became more refractory. The regeneration of the Pt catalyst did not completely eliminate the coke deposits, but these deposits hindered further formation of coke. A very different behavior was exhibited by the bimetallic catalysts. Both the oxidation and the regeneration procedures caused a large increase in the amount of coke that was formed during the subsequent 2-min cycles under reaction conditions.

Isobutane Dehydrogenation Activity

Isobutane dehydrogenation reaction studies were performed on the monometallic Pt and bimetallic Pt–Sn (CI), Pt–Sn (CIC), and Pt–Sn (SI) catalysts. Figures 12a and 12b compare the dehydrogenation activity and selectivity of the Pt (1.5), Pt–Sn (CI), Pt–Sn (CIC), and Pt–Sn (SI1) catalysts in a flow of isobutane : He, 2 : 1, at a space velocity of 248 WHSV. Although all bimetallic catalysts showed greater activity and selectivity than the unpromoted catalyst, the co-impregnated catalysts exhibited a significantly better performance than the sequentially impregnated catalyst. This superior performance was evident in the activity, selectivity, and stability. The selectivity of the co-impregnated

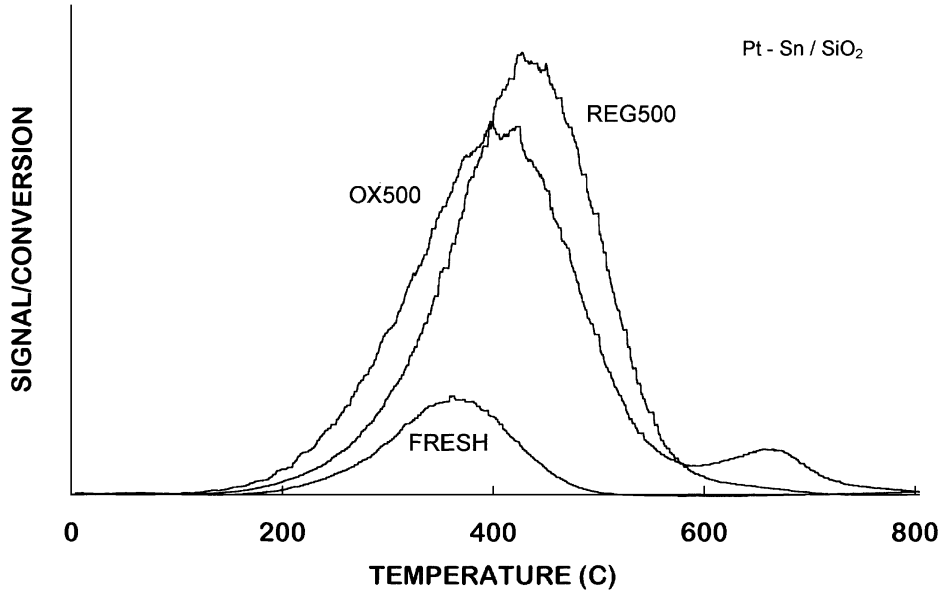

FIG. 11. TPO profiles of fresh, OX500, and REG500 sample of Pt–Sn (CI)/SiO_2 catalysts after exposure to isobutane at 500°C (248 WHSV) for 2 min.

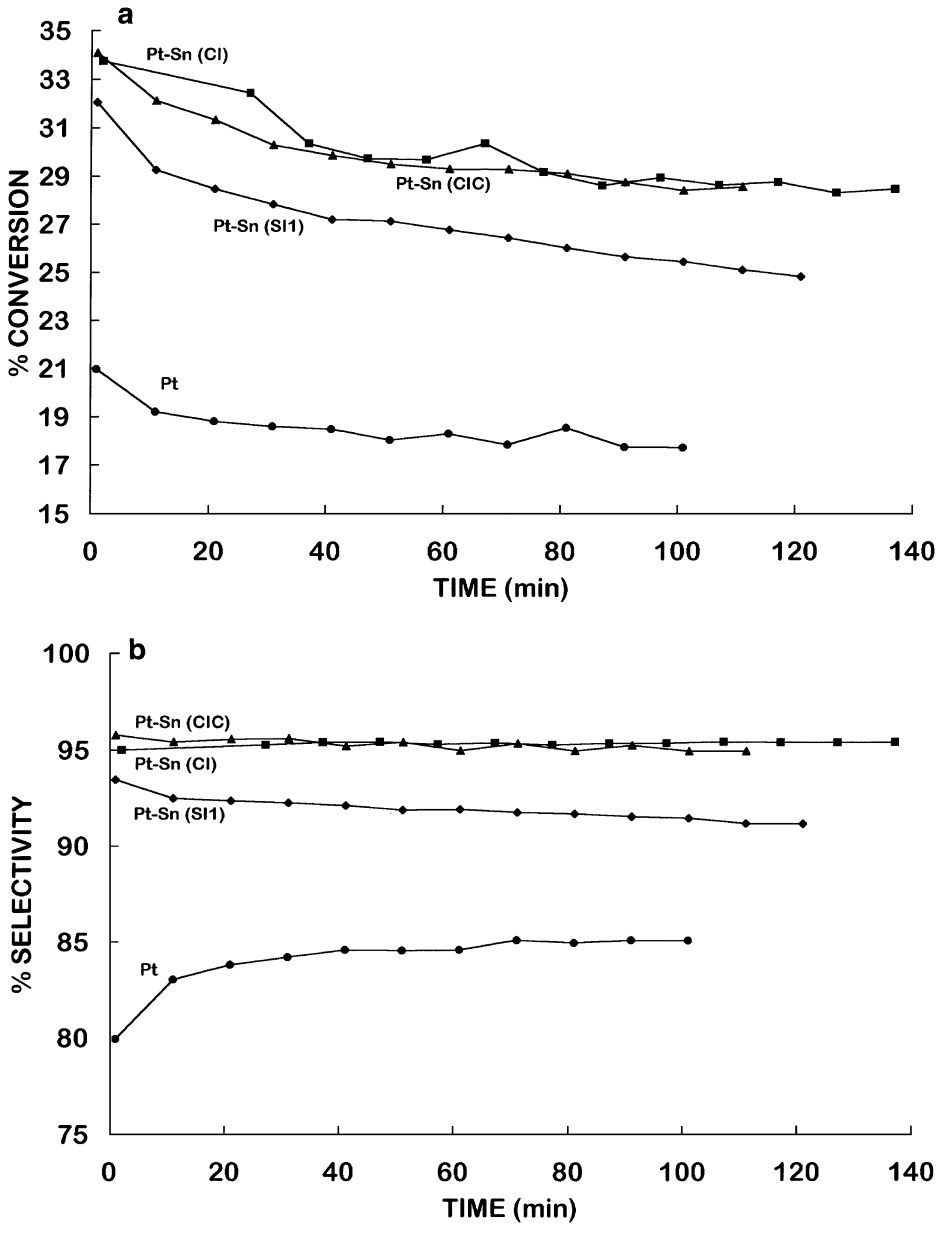

FIG. 12. Isobutane dehydrogenation as a function of time on stream over Pt (1.5), Pt–Sn (SI), Pt–Sn (CI), and Pt–Sn (CIC) catalysts in a flow of isobutane : He (2 : 1 ratio) at 500°C (248 WHSV). (a) conversion (%); (b) selectivity to isobutene (%).

bimetallics remained near 96% throughout the duration of the experiment, while the Pt (1.5) catalyst selectivity started at 80% and increased to reach a maximum of 84% after 100 min on stream. The sequentially impregnated catalyst presented a selectivity higher than the monometallic, but substantially lower than the co-impregnated catalysts.

The most dramatic differences displayed among the bimetallic catalysts prepared by the different procedures was observed when the samples were tested under pure isobutane at 500°C and a space velocity of 300 WHSV. Under these conditions the deactivation of the monometallic catalysts was very fast and the conversion after a few minutes was below the detectable limit. By contrast, no deactivation was observed on the Pt–Sn (CIC) catalyst which, under these conditions, maintained a 10% conversion for several hours and 100% selectivity to isobutylene. As illustrated in Fig. 13, the other co-impregnated CI catalyst exhibited similarly high conversion and selectivity. However, the rate of deactivation was significantly higher than that observed on the CIC sample. Finally, the sequentially impregnated catalyst exhibited a much poorer performance, with a conversion about one order of magnitude

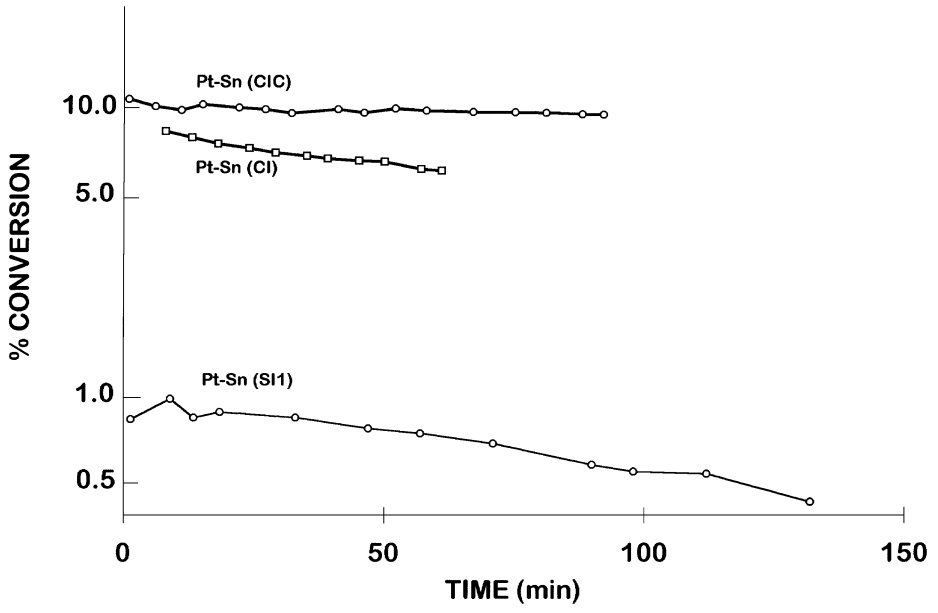

FIG. 13. Logarithmic comparison of the variation of isobutane conversion as a function of time for the Pt–Sn (CI), Pt–Sn (CIC) and Pt–Sn (Si1) in a flow of isobutane at 500°C (300 WHSV).

lower and, even at these low conversions, a high rate of deactivation.

Figure 14 shows the results of an experiment performed to analyze the effects of the presence of H_2 on the activity and selectivity of the bimetallic Pt–Sn (CIC) catalyst. In the first run, we exposed the sample to a flow of 10 cc/min isobutane and 110 cc/min He at a space velocity of 245 WHSV. Under these conditions, the catalyst exhibited a high initial activity but deactivated rapidly. A subsequent run was performed in the presence of H_2 keeping the same space velocity. In this run we used a flow of 10 cc/min isobutane, 100 cc/min He, and 10 cc/min H_2. In this case, the initial activity was much lower than that in the absence of H_2 but the deactivation was much less severe. After 90 min on stream,

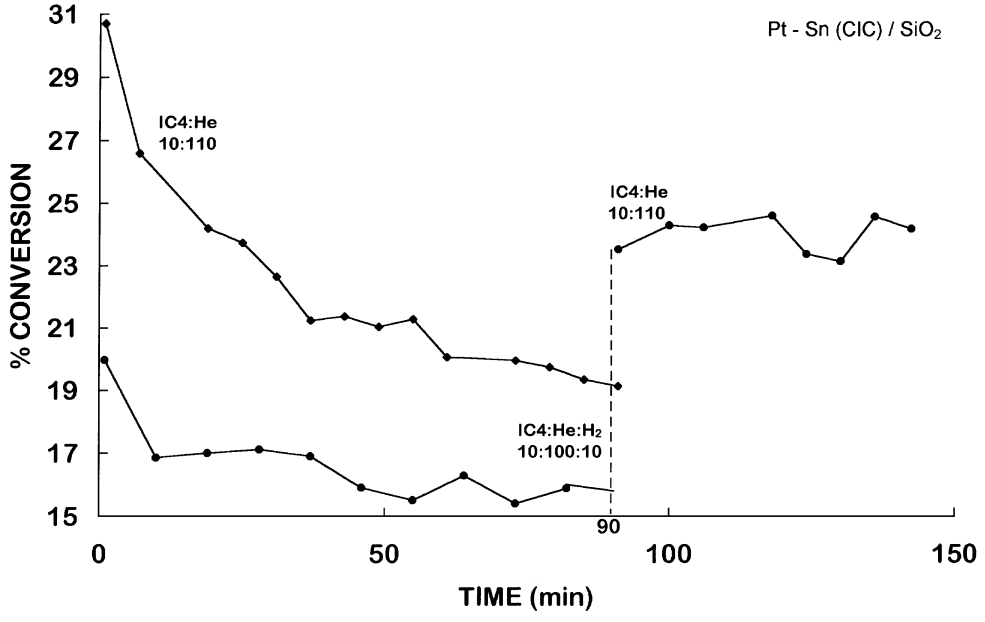

FIG. 14. Effect of hydrogen addition on the time evolution of the isobutane dehydrogenation activity of a fresh Pt–Sn (CIC) sample at 500°C. Circles, run in an isobutane : He mixture at a 10 : 110 flow ratio and a space velocity of 245 WHSV. Diamonds run in isobutane : He : H_2 at flow of 10 : 100 : 10 (245 WHSV) for 90 min and then returned to the conditions of the first run, that is, flow of isobutane : He at 10 : 110 (245 WHSV).

the flow was switched to the conditions of the first run, and the conversion increased to values even greater than that on the catalyst that was not exposed to H_2. Similar experiments were also performed on the pure Pt (1.0) catalyst; however, in this case, the initial activity in the presence of H_2 was higher than that for the runs diluted only with He.

To study the effect of regeneration on the monometallic and bimetallic catalysts, the spent Pt (1.5) catalyst after a reaction period of 100 min at 500°C (2 : 1 isobutane : He, 248 WHSV) was regenerated by carbon burning in air for 1 h at 300 and 500°C with subsequent reduction for 1 h in H_2 at 500°C. Figure 15a shows that, in the case of the monometallic Pt (1.5) catalyst, the regeneration at 300 and 500°C resulted in a catalytic behavior similar to that of the fresh Pt (1.5) catalyst. Figure 15a also shows the activity data for the pure Pt sample after reduction followed by oxidation at 300 and 500°C (OX300 and OX500) and subsequent reduction at 500°C. On these samples, the level of activity after 2 min was about the same as that of the fresh or regenerated samples, but, as opposed to the regenerated catalysts, these samples exhibited a dramatic increase in the rate of deactivation. After 90 min on stream, the catalysts had lost approximately 50% of their respective activities at 2 min.

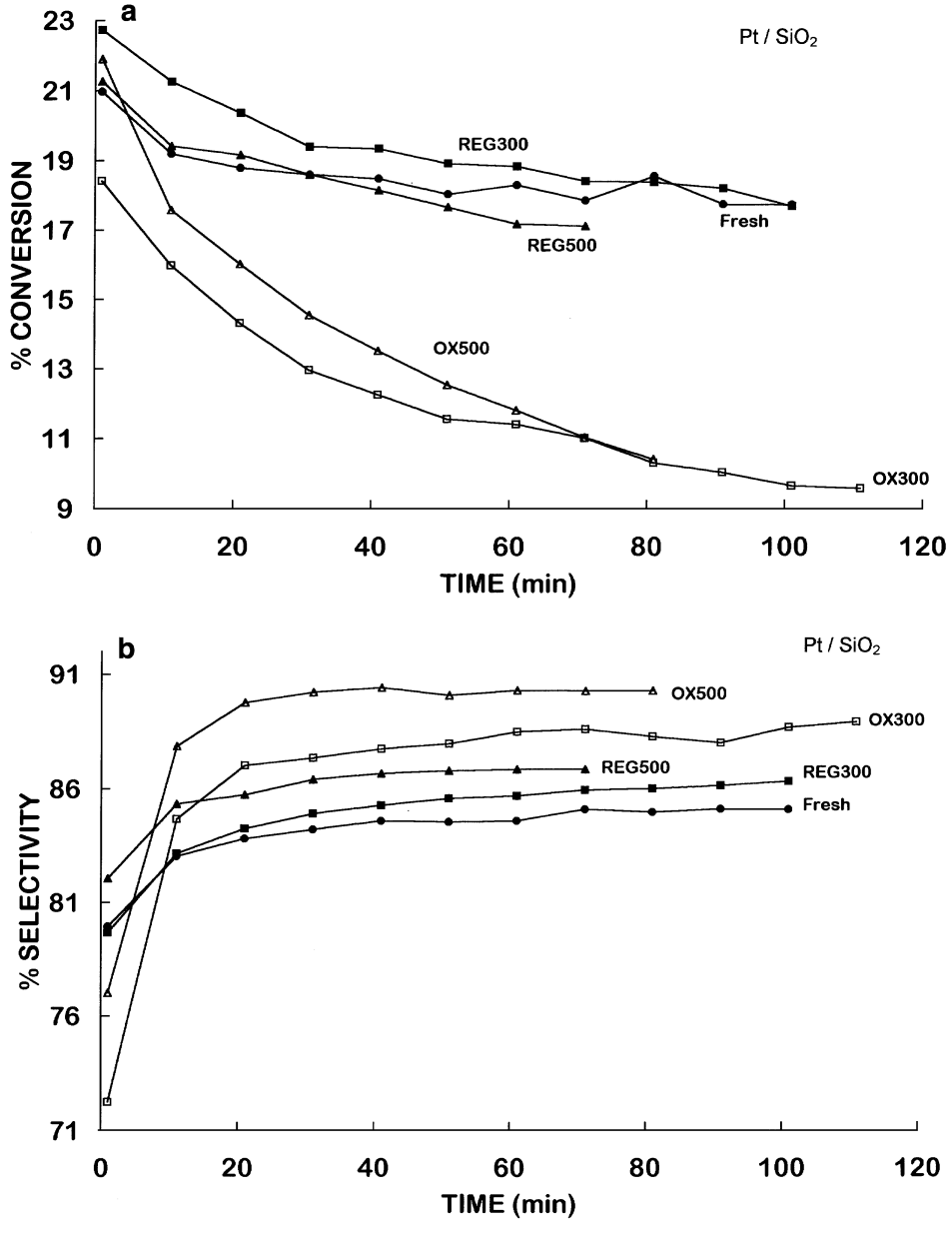

FIG. 15. Isobutane dehydrogenation as a function of time on stream over fresh, REG300, REG500, OX300, and OX500 samples of pure Pt (1.5) in a flow of isobutane : He (2 : 1 ratio) at 500°C (248 WHSV). (a) conversion (%); (b) selectivity to isobutene (%).

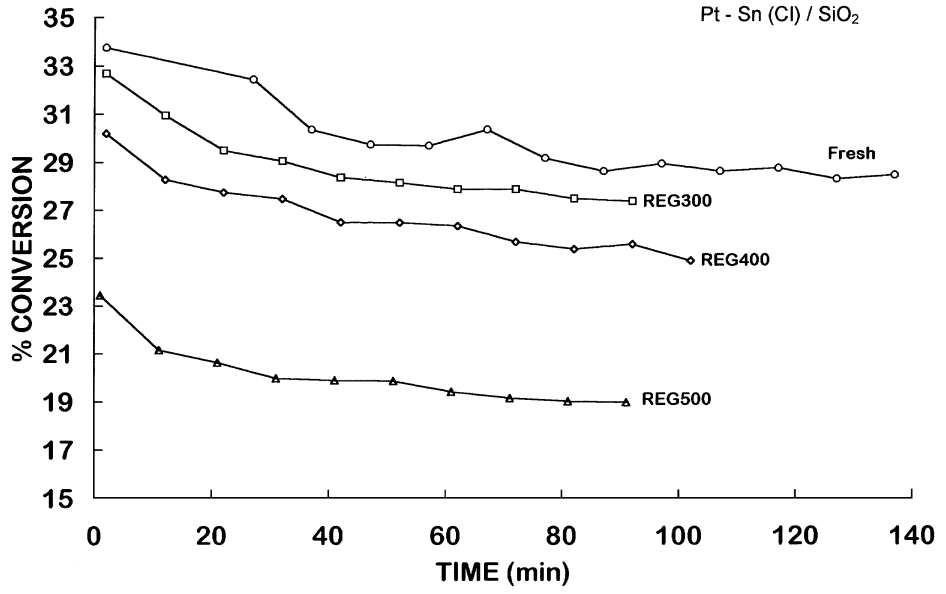

FIG. 16. Isobutane dehydrogenation activity for fresh, REG300, REG400, and REG500 samples of Pt–Sn (CI) in a flow of 2 : 1 isobutane : He at 500°C (248 WHSV).

The corresponding selectivity data for the same series of samples are shown in Fig. 15b. The fresh Pt sample had the lowest selectivity to isobutene when compared to the regenerated and oxidized catalysts. The regenerated catalysts had selectivities at 2 min near that of the fresh Pt, but then increased with time on stream to approximately 85%. Oxidation at 300 and 500°C resulted in an initial decrease in the selectivity, but after 10 min on stream the selectivity already reached 85% and continued to increase to values near 90%.

Figure 16 shows the effects of regeneration on the bimetallic Pt–Sn (CI) catalyst. The catalyst regenerated at 300°C regained almost all of the activity of the fresh catalyst. On the other hand, regeneration at 500°C resulted in a large loss of activity. The selectivity of the Pt–Sn (CI) catalyst showed only a slight decrease with regeneration. Figure 17 depicts the effects of the reduction/oxidation cycles on the Pt–Sn (CI) catalysts. The activity observed on the OX300 and OX500 samples was lower than the activity of the catalyst regenerated under the same conditions. Also, the

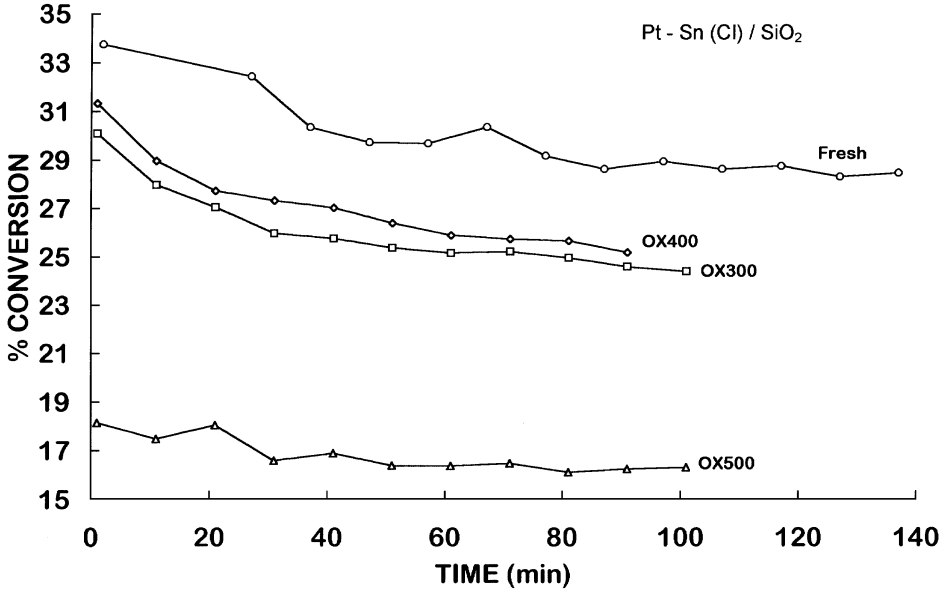

FIG. 17. Isobutane dehydrogenation activity for fresh, OX300, OX400, and Pt–Sn (CI) in a flow of 2 : 1 isobutane : He at 500°C (248 WHSV).

selectivities of all of the oxidized samples were lower than those of the regenerated samples at the equivalent temperatures. The catalytic behavior of the Pt–Sn (CIC) sample (not shown) did not differ much from that of the Pt–Sn (CI) sample described above. The main difference was a more pronounced drop in activity and selectivity after the regeneration treatment at 500°C.

In summary, although the bimetallic catalysts exhibited higher activity and selectivity than the monometallic ones, these differences became less pronounced after reduction/oxidation treatments at high temperatures. The high-temperature oxidation treatment had adverse effects on both monometallic and bimetallic catalysts, while the high-temperature regeneration only affected the catalytic behavior of the bimetallic samples.

DISCUSSION

The results presented in this contribution show the importance of the type of impregnation procedure used in the preparation of Pt–Sn/SiO_2 catalysts and demonstrate that the regeneration process may result in deterioration of the catalytic performance due to a decreased interaction between the active metal and the promoter.

Effect of the Impregnation Method Employed

The composition of the bimetallic clusters in Pt–Sn catalysts has been a matter of study for several years (26). The presence of bimetallic alloys has often been reported. For example, from their EXAFS and X-ray diffraction data, Meitzner *et al.* (6) have proposed that PtSn and Pt_3Sn alloys are present in reduced Pt–Sn catalysts. Similarly, Li *et al.* (27) used Mossbauer studies to show that PtSn is the most prevalent alloy formed on the bimetallic catalyst. Chojnacki and Schmidt (19) used TEM and electron diffraction to show that Pt and Sn supported on planar amorphous silica films consisted of several intermetallic species including PtSn, Pt_3Sn, and $PtSn_4$. Reduction of the films for 18 h at 650°C in H_2 resulted in particles with the major phase being PtSn but with a surface layer of $PtSn_4$. No FCC Pt was found on these films, possibly due to the long reduction times and high reduction temperatures. Although the oxidation state of Sn has been a matter of discussion, it is now widely accepted that the fraction of tin alloyed with Pt is metallic Sn^0 (28) and this fraction is much larger on SiO_2 than on Al_2O_3 (27, 29). Therefore, we could expect than on our SiO_2 support, depending on the initial distribution of the precursors on the surface, a relatively large amount of Sn should be alloyed with Pt.

In fact, the different TPR results obtained for the various preparations can be explained in terms of the presence of Pt–Sn alloys of different compositions (19, 30). The position of the reduction peaks can be expected to shift to higher temperatures as the concentration of Sn, more difficult to reduce than Pt, increases. For example, the Pt–Sn (CIC) sample showed two distinct hydrogen consumption peaks. The low-temperature reduction peak at around 125°C is characteristic of unalloyed Pt and was also seen on the monometallic Pt catalyst. The dominant peak at about 200°C can be ascribed to a Pt–Sn alloy with a higher concentration of Sn than those observed on the Pt–Sn (CI) sample, which had H_2 consumption peaks appearing at lower temperatures. In both cases, however, peaks indicative of unalloyed Sn, which should appear at much higher temperatures, were not observed. By contrast, the sequentially impregnated catalyst, Pt–Sn (SI), exhibited high-temperature consumption peaks. In this case, the Pt species are much less effective in catalyzing the reduction of Sn, indicating that a large fraction of Sn is physically separated from Pt. These results demonstrate that, among the preparation methods studied here, the co-impregnation methods are clearly superior to the sequential impregnation method. Preparations based on sequential impregnation methods may result in low extents of Pt–Sn interaction. For example, in agreement with our data, Barias *et al.* (15) have reported TPR profiles of Pt–Sn catalysts prepared by sequential impregnation that show large H_2 consumptions at high temperatures, indicating a large fraction of unalloyed Sn. If, as discussed below, the catalytic performance is a strong function of the extent of metal–metal interaction, the sequential impregnation method is not recommended.

The hydrogen and CO chemisorption data also support the conclusion that on the CIC sample there is a larger extent of Pt–Sn interaction than on the CI sample. Even though both bimetallic catalysts showed a decrease in the ability to adsorb hydrogen and CO when compared to the monometallic sample, the Pt–Sn (CIC) sample has a much lower adsorption capacity, corresponding to a higher degree of Pt–Sn interaction. A similar drop in chemisorption capacity has been observed by Cortright and Dumesic (31), who found that increasing the Sn loading resulted in a decrease in the fraction of exposed sites and a weakening of the hydrogen adsorption strength.

Effect of the Pt–Sn Interaction on Dehydrogenation Activity

The extent of metal–metal interaction resulting from the different preparations greatly affects the catalytic performance. One of the most obvious effects that we observed when adding Sn was an improvement in selectivity and stability compared to the monometallic Pt catalyst, even in the absence of H_2 in the feed.

These increases in stability and selectivity have been generally explained (4, 5) in terms of dilution of Pt ensembles by Sn, which greatly reduces the activity toward reactions that require a large ensemble of Pt atoms to constitute the

active sites, such as hydrogenolysis and coking. Also, the increase in selectivity of the pure Pt sample with time on stream can be explained by the same geometric arguments. The carbon deposits play the role of the inactive species that inhibit further undesired reactions. This explanation accounts for two observations on the pure Pt catalyst. Both the selectivity and the stability of the catalyst improve as a function of time on stream as the number of large ensembles in reduced by the presence of carbon.

On the pure Pt catalyst the initial deactivation is very fast. Thus, it is difficult to measure the "true" initial activity and determine whether the initial dehydrogenation rate on Pt is higher or lower than on the bimetallic catalyst. Some authors have reported that pure Pt is initially more active but after a short time it deactivates while the bimetallic retains its activity (32). Other authors have reported lower activities for the monometallic catalyst. It is conceivable that, in the catalysts prepared by sequential impregnation, the fraction of unalloyed Pt that rapidly deactivates is large enough to show a much lower initial rate than those prepared by co-impregnation. For the latter, the fraction of unalloyed Pt would be less and, as a consequence, they would present a lower extent of rapid deactivation.

The TEM micrographs in Figs. 1a and 1b show that the bimetallic catalyst contains large (250 Å) particles. As stated before, we believe that these particles are a combination of several Pt–Sn alloys. Even though the bimetallic catalysts, which have a high degree of interaction, are composed of these large particles, they still exhibited higher initial activity than the pure Pt catalyst which had much smaller particles (see Fig. 12). It is then clear that the catalytic activity that will result after the first few minutes on stream is not determined by the fraction of Pt exposed, i.e., the metal particle size, but rather by the degree of interaction between the metal and the promoter. The catalysts which have less interaction have a higher fraction of unalloyed Pt. As shown in Fig. 13, the Pt–Sn (SI) catalyst, which had the lowest extent of Pt–Sn interaction, exhibited a very high rate of deactivation, much greater than that of the Pt–Sn (CI) or (CIC) catalysts.

The notion that rapid deactivation is responsible for the apparent increase in initial activity with the addition of Sn is supported by the results of activity studies performed in the presence of hydrogen. Figure 14 clearly shows that the presence of hydrogen decreases the initial activity of the bimetallic catalyst. However, even though the initial activity of the catalyst decreases, the stability of the catalyst is increased because the presence of hydrogen increases the resilience to coke formation by cleaning the Pt surface (see Fig. 9). On the other hand, the results for the pure Pt catalyst show that the addition of H_2 resulted in increases in both initial activity and stability. On this catalyst, the coke removal capacity of hydrogen overcomes the decrease in activity by adsorption site competition. As a result, the reduction in deactivation rate manifests itself as an apparent increase in initial activity.

Although the geometric modification of the Pt ensembles by addition of Sn may explain most of the observed changes in catalytic properties, there are some indications that more subtle ligand effects may also be present. For example, the shape of the white line in the Pt L_{III} XANES spectra, representing allowed transitions from occupied 2*p* orbitals to unoccupied 5*d* orbitals is significantly altered by addition of Sn. This modification has been explained in terms of a transfer of electrons from Sn to Pt which would reduce the number of unfilled *d* states in Pt and could have an effect on the intrinsic catalytic properties. More recently, on the basis of a comparison of several intermetallic compounds (Pt_3M, where M = Ti, Co, or Sn), Ross (33) postulated that the intermetallic interaction is predominantly through *sp* orbitals rather than through *d* orbitals. In the case of Pt_3Sn alloys, the Pt–Sn bonding would involve the occupied Sn5*p* and the unoccupied Pt6*p*. The resulting donation of *p* electrons from Sn to Pt would only have an indirect effect on the *d* states of Pt, which would shift to lower energies and become narrower.

Even though the Pt–Sn interaction is relatively subtle, it can result in a decrease in the heat of CO adsorption as large as 20 kJ/mol (34). This energy difference would cause dramatic changes in the adsorption equilibrium constants at 298 K and, consequently, in the observed adsorption capacity. For example, a simple calculation can be done assuming that, at room temperature and under the dynamic adsorption conditions, the CO surface coverage should be significantly less than 1. Accordingly, a lowering of 20 kJ/mol in heat of adsorption represents a drop in coverage by a factor of 3.2×10^3.

If we analyze the CO adsorption data in Table 3, we can see that although the spent catalysts were still active after 1 h on stream, their CO adsorption capacity approached zero. As discussed above, the unalloyed Pt should be rapidly covered by coke while the Pt–Sn alloys remain more or less free of coke. We can conclude that the alloyed Pt does not adsorb significant amounts of CO and, therefore, the CO/Pt measured on the fresh catalyst is mainly due to the fraction of unalloyed Pt. The situation may be similar for the H_2 chemisorption. In fact, Verbeek and Sachtler (7) have shown that Pt–Sn alloys adsorb very little hydrogen and have ascribed this decrease to a lowering of the heat of adsorption. Recent microcalorimetry studies (5, 28, 29) showed that, even though the addition of Sn resulted in a large decrease in the saturation H or CO adsorption coverages, the heats of adsorption at zero coverage on Pt : Sn (1 : 1) samples were similar to those on pure Pt. However, it must be noted that these SiO_2-supported samples were prepared by sequential impregnation and, as shown above, this technique leads to a large fraction of unalloyed Pt. The adsorption that is measured under the conditions of those

studies occurs primarily on the Pt sites which are not forming an alloy with Sn. For changes in the initial heats of adsorption to be seen, a large fraction of Pt would need to be alloyed with Sn. When higher Sn concentrations were used in those studies, the heats of adsorption at zero coverage decreased significantly, as expected.

This conclusion has important consequences on the meaning of turnover frequencies on Pt–Sn catalysts. For example, if we compare the TOF based on both CO and hydrogen chemisorption for the pure Pt and bimetallic Pt–Sn catalysts we observe that these values significantly increase in the order Pt < Pt–Sn (CI) < Pt–Sn (CIC). Being dehydrogenation a structure-insensitive reaction, geometric arguments alone would predict that the TOF should be about the same on the three catalysts. As explained above, it is difficult to determine the "true" initial activity because, even after only a couple of minutes under reaction conditions the catalyst is already partially deactivated. Using a H_2 : hydrocarbon ratio of 6 : 1, Cortright and Dumesic (5) have found TOF values for a 1 : 1 Pt : Sn catalyst that are very similar to that of the pure Pt catalyst. However, at those high H_2 : hydrocarbon ratios, the initial deactivation should be much less severe than in our case.

If, as proposed above, the initial deactivation increases with the amount of unalloyed Pt, we might expect that deactivation should follow the opposite order to that of the observed TOF, i.e., Pt > Pt–Sn (CI) > Pt–Sn (CIC), even when the true initial TOF was the same on the three samples. The unalloyed Pt in the sample, due to rapid deactivation, is not the species responsible for sustained activity. However, CO and H_2 chemisorption primarily occurs on the unalloyed Pt. Therefore, for bimetallic Pt–Sn catalysts, TOF values based on CO or H_2 chemisorption have no practical significance.

Effect of Regeneration Procedures

As mentioned above, lower alkane dehydrogenation catalysts require frequent regenerations in air at high temperatures. These treatments can be detrimental to the dispersion of the metal and the interaction between the metal and promoter (35). In this work, we have investigated the effects of such treatments on the performance of Pt–Sn/SiO_2 catalysts.

As shown in the TPRs of Fig. 3, when the SI sample was treated in air at 500°C for increasing periods of time, the H_2 consumption peak associated with Pt–Sn alloy significantly decreased while those ascribed to unalloyed Pt and unalloyed Sn increased. This segregation was also observed in the co-impregnated catalysts which started with a much higher extent of Pt–Sn interaction. As shown in Fig. 4, the TPR peak at intermediate temperatures decreased with increasing oxidation temperature while the consumption at lower (Pt-rich) and higher (Sn-rich) temperatures gradually increased. Finally, a similar segregation phenomenon was observed when the coked catalyst was regenerated at 500°C in air. In this case, the splitting of the peaks was even more pronounced (see Fig. 5). It is interesting to consider the important differences observed in the TPR profiles of the samples of the OX (and REG) series with those that we call "fresh." One can note that, even though the fresh samples were oxidized at 400°C and then reduced at 500°C, they were clearly different from those of the OX and REG series which had an extra oxidation and reduction cycle.

TEM can also be used to support the segregation theory. Previous TEM studies on Pt–Sn (19) have found that oxidation at 550°C for 1 h resulted in severe morphological changes in the intermetallic particles. The Sn in the alloys formed on oxide and migrated to the surface of the particle. SnO_2 formed a ring around the edge of the particle in contact with the SiO_2 support. The Pt did not form an oxide but went to FCC Pt at the core of the particle. Subsequent 18-h reduction (650°C) resulted in complete recombination of the alloys. In our case, the TEM of OX500 after reduction for 1 h shows heterogeneous particles that are not present in the TEM of the fresh sample. We postulate that some recombination of the alloy may have occurred but that short reduction times after oxidation are not sufficient for total recombination of the alloy, leaving a particle with segregated Pt and Sn regions.

It is important to determine whether the proposed disruption of the alloys and metal segregation phenomena have an important effect on the catalytic properties. In fact, as demonstrated in this work, the effects may certainly be dramatic. Figure 11 shows that the reduction/oxidation treatment resulted in a large increase in the amount of coke deposited on the Pt–Sn (CI) sample. At the same time, the alloy disruption caused by the oxidation treatment resulted in an important drop in conversion as illustrated in Fig. 17 for the co-impregnated Pt–Sn (CI) sample.

The oxidation and regeneration treatments also altered the monometallic Pt catalyst, but the effects were different from those on the Pt–Sn samples. For example, the amount of coke deposited during 2 min in isobutane on the oxidized Pt catalysts was about the same as that deposited on the fresh catalyst. However, the TPO shows that on the former, the carbon deposits are more refractory. This change could be due to an increase in the Pt particle size, which are typically observed when Pt is heated in oxygen at high temperatures (36). However, as shown in Table 3 the change in chemisorption capacity was not very pronounced. It is possible that even though the overall metallic area did not change much upon the reduction/oxidation cycle, the type of exposed crystallographic planes changed, causing a change in the coking process. Studies on model Pt catalysts (37) have shown that graphitic carbon deposition occurs much more readily on flat terraces than on edges and corners. Therefore, if the reduction/oxidation cycle results in an increase in the density of flat planes, we might expect an increase in deposition of graphitic carbon.

As opposed to the reduced/oxidized samples, the regenerated monometallic Pt catalysts showed less coke than the corresponding fresh samples. This result can again be explained in terms of the presence of refractory carbon deposits left on the surface after the regeneration which can act as diluting species breaking up Pt ensembles and reducing the rate of coke formation.

The observed trend in coke formation on the monometallic catalysts was paralleled by that of the rates of deactivation. The oxidized monometallic samples, which exhibited a high rate of coke formation, showed a much higher rate of deactivation than the fresh and regenerated catalysts and a more pronounced variation in selectivity. Also, the initial selectivity was lower for the OX500 sample than for the other two samples, which is consistent with the presence of flat Pt planes, more active for hydrogenolysis and coke formation. This sample rapidly formed coke so it deactivated and increased selectivity more rapidly than the other two samples.

The activity studies showed that both the oxidation and the regeneration of the bimetallic Pt–Sn catalysts at 500°C resulted in a great loss of activity and selectivity. The decrease in activity can be due to segregation or partial destruction of the Pt–Sn alloy which results in an increase in the deactivation due to coking. Comparison of the TPO profiles for the fresh and OX500 Pt–Sn (CI) with that for the fresh and OX500 Pt samples show that after oxidation at 500°C a high-temperature carbon peak forms as in the case of OX500 Pt. This could indicate that some of the alloy has been destroyed leaving behind patches of unalloyed Pt, on which the formation of the graphitic carbon is more favorable. The OX500 and REG500 bimetallic Pt–Sn (CI) samples still form less carbon than the pure Pt sample, but almost four times the amount found on the fresh bimetallic sample. Comparison of Figs. 16 and 17 shows that the REG500 bimetallic sample Pt–Sn (CI) retained more of its initial activity than the OX500 sample. This difference can be explained by the same argument used above for the monometallic catalyst, the carbon not removed during the regeneration hinders the coke formation on the unalloyed Pt regions.

To explain the changes in catalytic activities and properties experienced by the Pt–Sn (CI) and Pt–Sn (CIC) catalysts after reduction/oxidation cycles and regeneration at 500°C we may not need to postulate the complete segregation of the metals in separate particles. Based on the surface enrichment model observed on the Pt–Sn and the Pt–Rh alloys and the TEM evidence of Chojnacki and Schmidt (19), we can speculate that, after reduction and before the treatment in air, the particle is composed of a Pt–Sn alloy. Under oxidizing conditions at high temperatures, the Sn forms an oxide and, at the expense of the subsurface layer, the exterior becomes rich in Sn. The Pt, which does not form an oxide, is metallic and becomes the core of the particle. Reduction at high temperatures results in the destruction of the oxide and possibly redistribution of the Sn, opening patches of pure Pt. Although the thermodynamically most stable configuration would be the complete recombination of the alloy (7, 19), short reduction times do not allow for this to occur. Consequently, after reduction, the bimetallic particles have become heterogeneous, with Sn-rich regions interdispersed with Pt-rich regions. It is even possible that pure Pt ensembles are present allowing for the formation of more refractory carbon to form on the surface under subsequent exposure to reaction conditions. The dramatic consequences of the reduction/oxidation treatments on the catalytic properties of silica-supported Pt–Sn catalysts demonstrated in this work should be taken into account when the regenerability of a dehydrogenation catalyst is considered for practical applications.

CONCLUSIONS

In this contribution we have shown that the addition of Sn can significantly improve the catalytic behavior of Pt/SiO_2 catalysts for the dehydrogenation of isobutane conducted under severely deactivating conditions, i.e., at 500°C and without the addition of hydrogen. The main conclusions of this study are the following:

- The promoting effect of Sn strongly depends on the method employed in the preparation. Catalysts prepared by co-impregnation, particularly when the solvent is an aqueous solution containing HCl, result in a high extent of Pt–Sn interaction. By contrast, sequential impregnation results in a large fraction of unalloyed Pt. When H_2 is not added to the feed, this fraction of unalloyed Pt rapidly deactivates.
- In choosing a preparation method, one needs to maximize the degree of Pt–Sn interaction rather than maximizing the metal dispersion because it is the fraction of alloyed Pt the one that will be responsible for the sustained activity.
- High-temperature treatments in air of previously reduced Pt–Sn samples are detrimental for the catalytic properties. After these treatments, the rate of deactivation due to coke formation greatly increases. It is postulated that a Pt–Sn segregation resulting in disruption of the alloy structure is responsible for this effect. Reduction after oxidation results in some recombination of the alloy, but long times and high temperatures are necessary for complete recombination.
- CO and hydrogen adsorption does not take place to a great extent on the Pt–Sn alloys, the small amount measured occurs mostly on unalloyed Pt. Since, in the absence of added H_2, this fraction of the catalyst is rapidly deactivated, TOF values based on H/Pt or CO/Pt values have no practical significance.

ACKNOWLEDGMENTS

We gratefully acknowledge the Donors of the Petroleum Research Fund administered by the American Chemical Society and the NSF-CONICET International Program (INT-9415590) for their generous support. We thank NSF for a traineeship (SMS). We thank Micromeritics for the donation of a ASAP2000 adsorption apparatus. We thank the University of Mar del Plata for a fellowship for one of us (WEA), as part of the international exchange program sponsored by the University of Oklahoma and the University of Mar del Plata. We also thank the Japanese International Cooperation Agency (JICA) for their support of INCAPE, Argentina.

REFERENCES

1. Resasco, D. E., and Haller, G. L., *in* "Catalysis," Vol. 11, p. 379. Royal Chem. Soc., London, 1994.
2. Yarusov, I. B., Zatolokina, E. V., Shitova, N. V., Belyi, A. S., and Ostrovskii, N. M., *Catal. Today* **13**, 655 (1992).
3. Yang, W., Lin, L., Fan, Y., and Zang, J., *Catal. Lett.* **12**, 267 (1992).
4. Dautzenberg, F. M., Helle, J. N., Biloen, P., and Sachtler, W. M. H., *J. Catal.* **63**, 119 (1980).
5. Cortright, R. D., and Dumesic, J. A., *J. Catal.* **148**, 771 (1994).
6. Meitzner, G., Via, G. H., Lytle, F. W., Fung, S. C., and Sinfelt, J. H., *J. Phys. Chem*. **92**, 2925 (1988).
7. Verbeek, H., and Sachtler, W. M. H., *J. Catal.* **42**, 257 (1976).
8. Paffett, M. T., Gebhard, S., Windham, R. G., and Koel, B. E., *Surf. Sci.* **223**, 449 (1989).
9. Xu, C., Koel, B. E., and Paffett, M. T., *Langmuir* **10**, 166 (1994).
10. Antos, G. J., U.S. Patent 4,216,346, 1980.
11. Olbrich, M. E., McKay, D. L., and Montgomery, D. P., U.S. Patent 4,926,005, 1986.
12. Catalytica Studies Division, *in* "Catalytic Dehydrogenation and Oxidative Dehydrogenation." Catalysis Studies No. 4190 DH, 1991.
13. Chojnacki, T. P., and Schmidt, L. D., *J. Catal.* **115**, 473 (1989).
14. Wang, T., and Schmidt, L. D., *J. Catal.* **70**, 187 (1981).
15. Barias, O. A., Holmen, A., and Blekkan, E., *Catal. Today* **24**, 361 (1995).
16. Chen, M., and Schmidt, L. D., *J. Catal.* **56**, 198 (1979).
17. Foger, K., and Jaeger, H., *J. Catal.* **70**, 53 (1981).
18. Sinfelt, J. H., and Via, G. H., *J. Catal.* **56**, 1 (1979).
19. Chojnacki, T. P., and Schmidt, L. D., *J. Catal.* **129**, 473 (1991).
20. Nuñez, G. M., and Rouco, A. J., *J. Catal.* **111**, 41 (1988).
21. Resasco, D. E., Marcus, B. K., Huang, C. S., and Durante, V. A., *J. Catal.* **146**, 40 (1994).
22. De Miguel, S. R., Baronetti, G. T., Castro, A. A., and Scelza, O. A., *Appl. Catal.* **45**, 61 (1988).
23. Fung, S., and Querini, C. A., *J. Catal.* **138**, 240 (1992).
24. Balakrishnan, K., and Schwank, J., *J. Catal.* **127**, 287 (1991).
25. Afonso, J. C., Aranda, D. A. G., Schmal, D., and Frety, R., *Fuel Proc. Technol.* **42**, 3 (1995).
26. Srinivasan, R., and Davis, B. H., *Platinum Metals Rev.* **36**, 151 (1992).
27. Li, Y. X., Klabunde, K. J., and Davis, B. H., *J. Catal.* **128**, 1 (1991).
28. Lieske, H., and Volter, J., *J. Catal.* **90**, 46 (1984).
29. Zhou, Y., and Davis, S. M., *Catal. Lett.* **15**, 51 (1992).
30. Chang, T.-H., and Leu, F. C., *J. Chin. Inst. Chem. Eng.* **26**, 393 (1995).
31. Cortright, R. D., and Dumesic, J. A., *Appl. Catal. A* **12**, 101 (1995).
32. Cortright, R. D., and Dumesic, J. A., *J. Catal.* **157**, 576 (1995).
33. Ross, P. N., *J. Vacuum. Sci. Technol.* **10**, 2546 (1992).
34. Haner, A. H., Ross, P. N., Bardi, U., and Atrei, A., *J. Vacuum Sci. Technol.* **10**, 2719 (1992).
35. Fan, Y., Xu, Z., Zang, J., and Lin, L., *in* "Catalyst Deactivation 1991." Elsevier, Amsterdam; *Stud. Surf. Sci. Catal.* **68**, 683 (1991).
36. Chen, M., and Schmidt, L. D., *J. Catal.* **55**, 348 (1978).
37. Somorjai, G. A., and Blakely, D. W., *Nature* **258**, 580 (1975).